

]]STATISTICAL CHARACTERISTICS OF THREE-COMPONENT TURBULENCE INTENSITIES FOR HIGH REYNOLDS NUMBER PIPE FLOW USING LDV

Marie Ono

National Metrology Institute of Japan
Advanced Industrial Science and Technology
1-1-1 Umezono, Tsukuba, Ibaraki, Japan
ono.marie@aist.go.jp

Noriyuki Furuichi

National Metrology Institute of Japan
Advanced Industrial Science and Technology
1-1-1 Umezono, Tsukuba, Ibaraki, Japan
furuichi.noriyuki@aist.go.jp

Yoshiyuki Tsuji

Graduate school of engineering
Nagoya University
Furocho, Nagoya, Aichi
c42406a@cc.nagoya-u.ac.jp

ABSTRACT

In this study, we report three components (streamwise, wall-normal and spanwise) turbulence intensity profiles from $Re_\tau = 990$ to $Re_\tau = 20750$ using laser Doppler velocimetry (LDV) at high Reynolds number actual flow facility (Hi-Reff). These profiles were measured by changing the angle of the measurement line and the angle of the beam with respect to pipe. The LDV specific issues such as the spatial resolution and the fringe distortion are considered to measure reliable experimental data. These issues that influences turbulence statistics are evaluated by a wire rotary device and reflected to the measurement by new correction method. The corrected results of 3 components turbulence intensity profiles agree well with the previous DNS data until $Re_\tau = 8000$ and with the previous experimental data at high Reynolds number. The streamwise and spanwise turbulence intensities grow including the peak values depending on Reynolds number up to $Re_\tau = 20750$. Moreover, streamwise inner peaks are good agreement with previous experimental results of TBL. On the wall-normal turbulence intensities measurement, the peak values asymptote to $(v'^+)^2 = 1.3$ with Reynolds number increases. The logarithmic region or constant region are clearly observed in 3 components for $Re_\tau > 11200$, The positions are same between streamwise and spanwise component ($y/R = 0.05 \sim 0.25$), but different with the wall-normal component ($y/R = 0.015 \sim 0.07$).

INTRODUCTION

To establish scaling laws of a mean velocity and turbulence intensity in a wall-bounded flow at high Reynolds number has studied by many researchers. Major concerns in a statistic of the turbulence intensity profile are an inner peak, an outer peak of streamwise component and an outer logarithmic region of 3 component behaviours at high Reynolds number. It is well known that the value of the inner peak increases with Reynolds number, but it has not been clarified whether it is finite/infinite. The scaling law for the inner peak is also still under discussion (Marusic et al. 2017, Chen and Sreenivasan, 2018). For the outer peak observed in high Reynolds number pipe flow, it is still not unclear whether it has somewhat physical meaning of the turbulence or it comes from measurement issue (Hultmark et al., 2012, Willert

et al., 2017). The logarithmic region in the outer region, which is based on attached eddy model (Perry & Chong, 1982), is clearly observed for the streamwise components at high Reynolds number, however, it has not been well discussed for the wall-normal and spanwise component including the position where it is emerged. High Reynolds number data is necessary to establish these scaling laws. However, the lack of reliable experimental data because large-scale facilities are required and we cannot avoid the issues from velocity measurement devices for high Reynolds number experiments.

The main objective of this study is to establish the scaling law for the turbulence intensity profile of three components. To this end, the issues for the measurement devise, which is laser Doppler velocimetry (LDV), are well considered especially for the spatial resolution and the fringe distortion, applied new approach to correct the results measured at high Reynolds number (Ono et al. 2022). Based on those precise measurement, we discuss on the Reynolds number dependency of the streamwise inner peak and the logarithmic behaviour of three-component turbulence intensity profiles in the pipe flow.

LDV SPECIFIC ISSUES

While LDV has relatively higher spatial resolution than other methods for velocity measurement and can measure at near the wall, however, it has several issues to achieve the

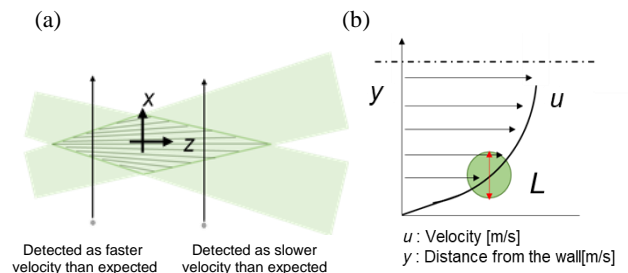


Figure 1. (a) The fringe distortion in LDV measurement and (b) The effects of finite the control volume (spatial resolution).

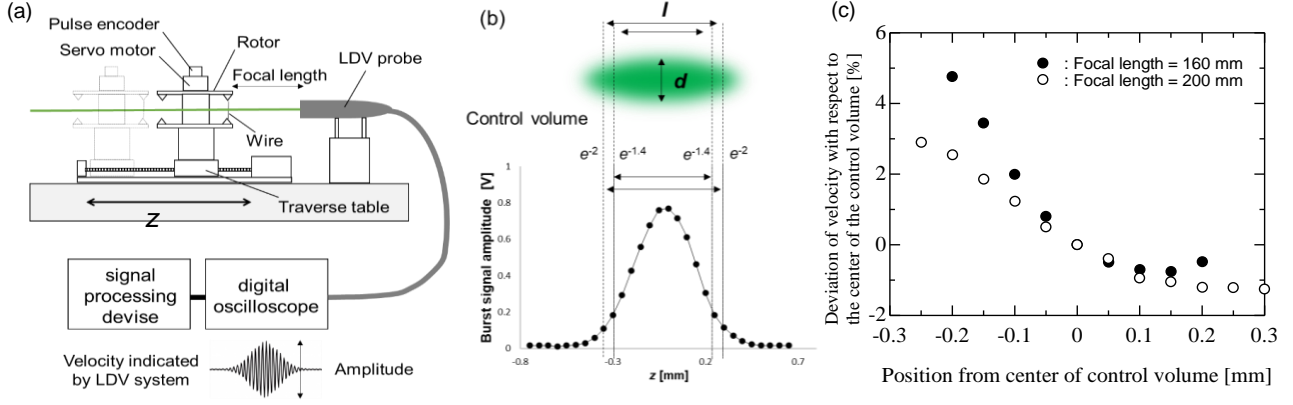


Figure 2. (a) Wire rotary device, (b) Distribution of burst signal amplitude and determination of the control volume size, (c) Influence of fringe distortion on different focal length.

precise measurement. In this paper, two important issues, which are the fringe distortion (Fig. 1(a)) and the spatial resolution (Fig. 1(b)) for measurement, are focused since those are critical factors for high Reynolds number measurement. The fringe distortion may strongly influence to the turbulence intensity at the outer region. On the other hand, the spatial resolution derived the size of the control volume may strongly influence to it at the inner region where has large velocity gradient, especially the value of the inner peak. Those influences of LDV have been pointed out in the previous, however, there is no established correction methods especially for high Reynolds number.

In this experiment, a wire rotary device (Fig.2(a)) was used to obtain detail information of the size of the fringe spacing and the control volume. The absolute velocity of LDV was calibrated based on the rotating speed of the tungsten wire attached to the rotor. By the traversing the rotor, the velocity at each position in the control volume can be obtained. In Fig.2(c), the deviation from the velocity at the centre in the control volume is investigated. This result is clear evidence that the fringe distance is distorted, namely fringe distortion. The turbulence intensity is overestimated by this fringe distortion because particles which have same velocity are

detected as different velocity depending on the passing position in the control volume. Thus, we apply new correction method based on the probability density function. The measured probability density function $P_M(u; V)$ of the velocity fluctuation is estimated by the integration of $P_A(u, z)$ over the control volume,

$$P_M(u; V) = \frac{1}{V} \int_{-l/2}^{l/2} P_A(u; z) s(z, V) dz, \quad (1)$$

where l is the major diameter of the control volume, $s(z, V)$ is the infinitesimal volume at the z position. $P_A(u; z)$ is expressed using base PDF P_B ,

$$P_A(u; z) = \frac{P_B\{[u - U(z)]/\sigma(z)\}}{\sigma(z)}, \quad (2)$$

where $U(z)$ is mean velocity and $\sigma(z)$ is standard deviation at z . With assuming the base PDF P_B is invariant in the control volume, $P_A(u; z)$ at the centre of the control volume can be estimated inversely to satisfy Eq.(1).

Contrary to hot wire measurements, the turbulence intensity at near wall is overestimated in LDV measurement due to the velocity gradient in the control volume. Durst et al. (1995) reported the following,

$$u_{meas}^2 = u_{cv}^2 + \frac{L^2}{16} \left(\frac{dU_{cv}}{dy} \right)^2 + \frac{L^2}{32} \left(\frac{d^2 u_{cv}^2}{dy^2} \right), \quad (3)$$

as the relation between the measured and the actual turbulence intensity at the center of the control volume. Where, u_{meas}^2 indicates the measured turbulence intensity in the control volume, U_{cv} and u_{cv}^2 are the mean velocity and turbulence intensity at the centre of the control volume, respectively. L is the actual length considered as the spatial resolution and it is important parameter for the precise measurement. The size of the control volume can be calculated from the optical and geometric parameters of LDV, however it does not give any guarantee for it in the actual measurement. In this presentation, the size of the control volume was obtained by the wire rotary device and the turbulence intensity measurement using three different spatial resolutions. As shown in Fig.2(b), the distribution of the burst signal amplitude is measured by the wire rotary device, and the major length l is determined by certain threshold of it. The threshold level is determined to

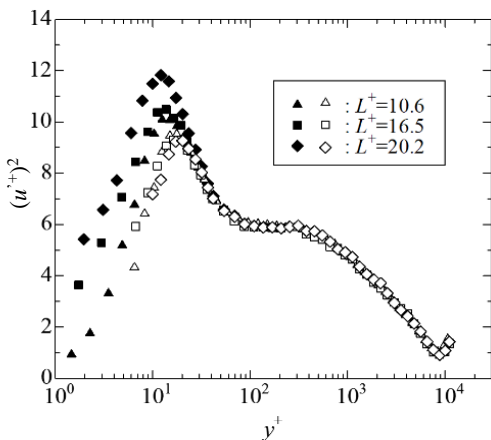


Fig. 3 The turbulence intensity profiles $Re_\tau=8610$ measured by three different control length L^+ ($L^+ = Lu_\tau/\nu$). Closed symbols are uncorrected results. Open symbols are corrected by Eq. (3).

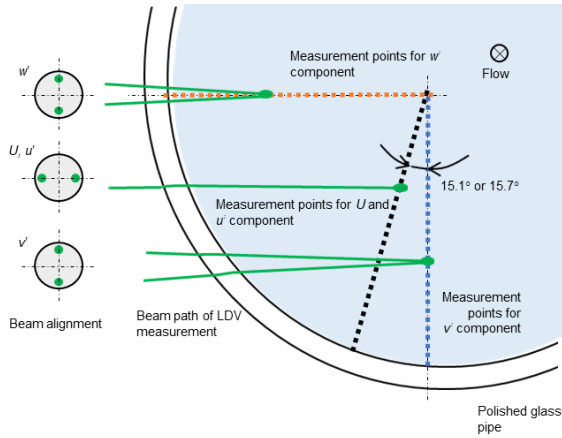


Figure 4. LDV Measurements of 3 components. Spanwise component was measured on the red dashed line, streamwise component was black, wall-normal component was blue.

take same value of the inner peak value among three different spatial resolutions. The minor axis d is determined by the formula $d = l \sin \phi / \cos \phi$ (ϕ is the half-intersection angle of the beams.). When the minor axis d and the major axis l are determined, the control length L is determined by them, another optical and geometrically conditions. Fig. 3 shows streamwise turbulence intensity profiles measured by three different spatial resolution. Turbulence intensities are overestimated by the control length L and this effect is significantly at near the wall. However, corrected by Eq. (3) profiles are consistency.

The correction of the fringe distortion and the spatial resolution were applied to 3 components. The effects of two issues are significant on streamwise component, but these

effects are small on spanwise and wall-normal components because velocities are low and the velocity gradient is small.

EXPERIMENT

Experiments for the fully-developed pipe flow at high Reynolds number was conducted in Hi-Reff. Water at ambient temperature was used as the working fluid. The range of Reynolds number was $Re_\tau=990-20750$. Notable features of this facility are steady flow by supplying from a head tank 30 m high and high accuracy flow rate measurement by static gravimetric methods (Furuichi et al., 2015). Measurement components are streamwise, wall-normal and spanwise. Each measurement was conducted by different insertion of laser beam as shown in Fig.4. The measurement line for streamwise component was slightly inclined (15.1-15.7deg) to measure at near the wall. The axisymmetric flow field was guaranteed from the pre-experiments and the reproducibility of Reynolds number was very high in Hi-Reff, which is less than 3% for each velocity component measurement.

RESULTS

Experimental results for the turbulence intensity profiles from $Re_\tau=990$ to $Re_\tau=20750$ are shown in Fig.5. All experimental data is corrected based on the proposed correction procedure above mentioned. In the same figure, the DNS results for the pipe and channel flow up to $Re_\tau=8000$ are also drawn to compare with the present results. For the streamwise component, inner peaks increase with Reynolds number increases. The present experimental results are very nice agreement with DNS result at $Re_\tau=1000$ and 2000. For higher Reynolds number, except the overlap region ($y^+=100 - 500$), the present results show nice agreement with DNS result. However, it should be noted that each DNS result shown in

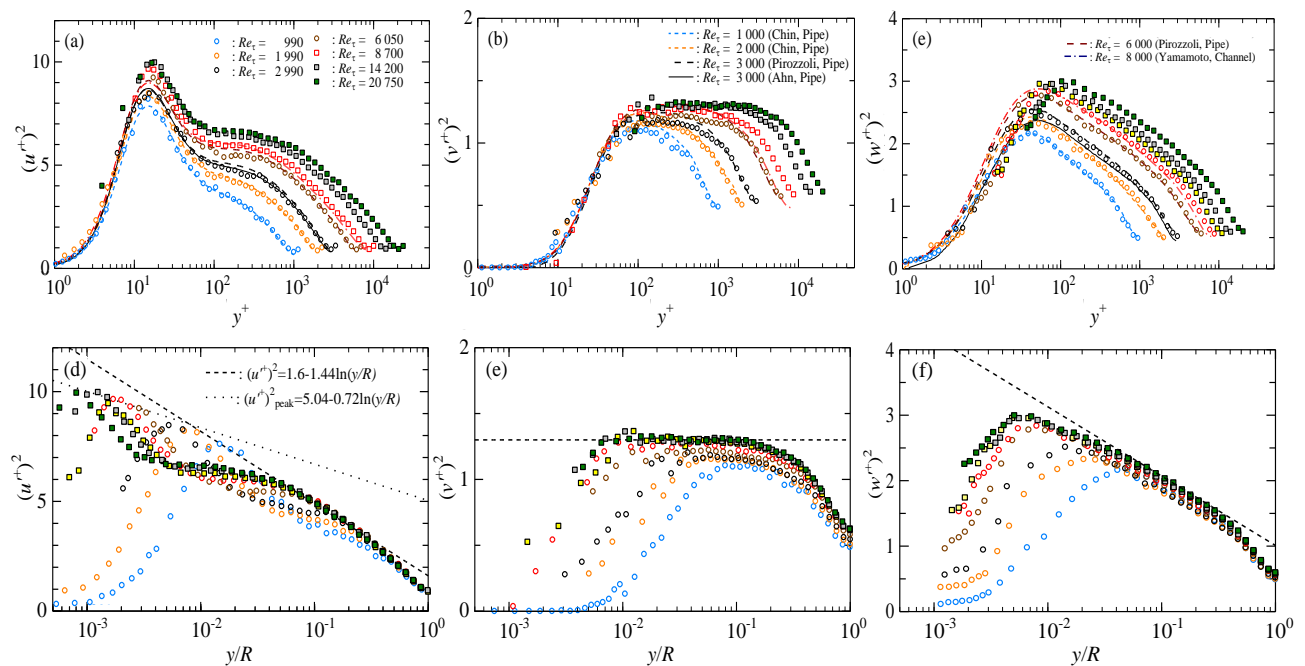


Figure 5. Comparison turbulence intensity profiles with previous DNS data. Upper figures show inner scaling and under figures show outer scaling. The black dotted lines in under figures show logarithmic or constant law related to attached addy hypothesis and these constants were determined by fitting from present results.

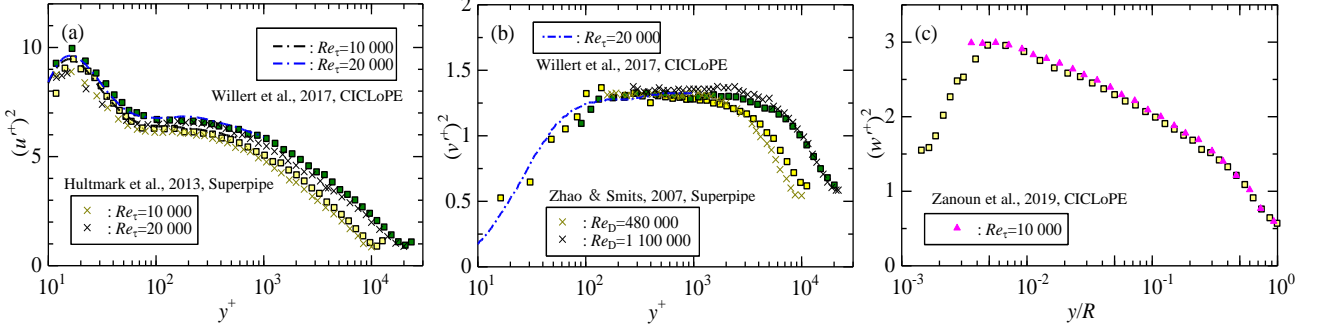


Figure 6. Comparison turbulence intensity profiles with previous experimental data at high Reynolds number pipe flow. Present results of $Re_\tau = 11200$ and 20750 show in these figures as same symbol with Fig. 5.

the figure have difference in the overlap region even though same Reynolds number. Further discussion for this inconsistency may be necessary. Regarding the outer peak, it was not observed even $Re_\tau=20000$.

For the wall-normal component, around the overlap region for low Reynolds number, the difference can be observed between the present and DNS results. Experimental turbulence intensity is smaller than DNS in this region. However, for higher Reynolds number region, the turbulence intensity around the overlap region shows nice agreement each other. The peak values asymptote to 1.3 with Reynolds number increases.

For the spanwise component, the peak values increase with Reynolds number. The results at low Reynolds number $Re_\tau = 1000$ and 2000 show nice agreement between the present and DNS. For higher Reynolds number up to $Re_\tau = 8000$, the outer region shows nice agreement, but the difference can be observed in the inner region. There is the difference of inner region between DNS data. Although the effect of the spatial resolution is small in other than streamwise, the inner peak of spanwise component need to be discussed in the future.

While small difference is observed as mentioned, the present turbulence intensity profiles for three components show high level consistency with DNS results. It is difficult to find such consistent result for three components in the previous studies. From this result in the low Reynolds number, the reliability in high Reynolds number region would increase. Here, we make attention to the logarithmic region around $y/R=0.1$ according to the previous studies (y is the wall-normal position and R is radius of the pipe). The turbulence intensity profiles based on the attached eddy model are the following,

$$u'^{+2} = B_{1,u} - A_{1,u} \ln(y/R) \quad (4)$$

$$v'^{+2} = B_{1,v} \quad (5)$$

$$w'^{+2} = B_{1,w} - A_{1,w} \ln(y/R) \quad (6)$$

Based on the detail analysis using indicator functions $\mathcal{E}_u = y^+ d((u^+)^2)/dy^+$, $\mathcal{E}_v = y^+ d((v^+)^2)/dy^+$, $\mathcal{E}_w = y^+ d((w^+)^2)/dy^+$, the clear logarithmic region for Eq.(4) and (6) can be found for $Re_\tau > 11200$ and $A_{1,u}$ has Reynolds number dependency while it expected to be universal constant. In this experiment, $A_{1,u}=1.44$, $B_{1,u}=1.60$, $B_{1,v}=1.3$, $A_{1,w}=0.46$, $B_{1,w}=-0.99$ are obtained at $Re_\tau = 20750$. It should be noted that the positions where Eq.(4)-(6) are satisfied is same between streamwise and spanwise component ($y/R = 0.05 \sim 0.25$), but different with the wall-normal component ($y/R = 0.015 \sim 0.07$). The constants involved in Eq.(4)-(6) are slightly different to

previous pipe data at high Reynolds number(Zhao & Smits, 2007, Hultmark et al., 2013, Zanon et al., 2019), however, these profiles show sufficient agreement with the present results (see Fig. 6).

The Reynolds number dependency of the inner peak value is shown in Fig.7. The error bars indicate the uncertainty calculated by the variation among three different spatial resolutions. The dotted line is the logarithmic scaling of the inner peak (Marusic et al., 2017) and the broken line is the asymptotic relation given by the expected dissipation ratio at the near wall (Chen et al. 2021).

$$(u^+)^2_{peak} = A_2 \ln Re_\tau + B_2 \quad (7)$$

$$(u^+)^2_{peak} = \alpha \left(\frac{1}{4} - \frac{\beta}{Re_\tau^{0.25}} \right) \quad (8)$$

The constants of Eq. (7) and Eq. (8) obtained from present results are $A_2 = 0.72$, $B_2 = 3.01$, $\alpha = 46$, $\beta = 0.44$. Both equations well represent the experimental results, while it seems that the present result is consistent with the later. The importance of the present result is the consistency with results in TBL. In the previous studies for the pipe flow, they take asymptotic values and widely scattered at high Reynolds number. However, the

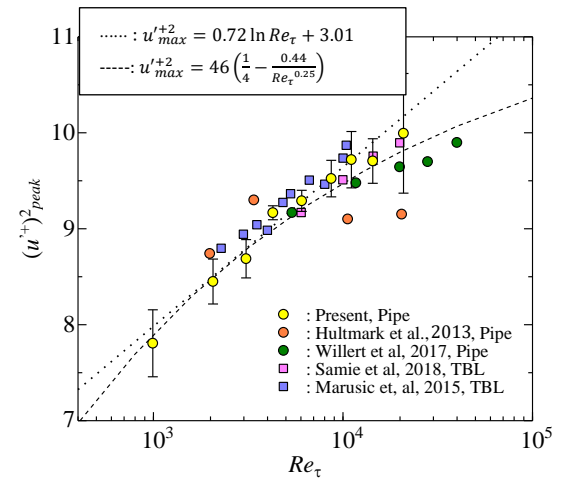


Figure 7. Comparison the Reynolds number dependency of streamwise inner peak with previous experimental data and Eq. (7) and Eq. (8). The constants of Eq. (7) and Eq. (8) were determined by fitting from present results.

present results do not take asymptotic value and well agreement with TBL results by Samie et al. (2018). The consistency indicates possibility that the streamwise inner peak values independence of the geometry. This result would come from the highly considered spatial resolution of the measurement.

Furthermore, it is reported that the relationship between Reynolds number dependence of inner peak and the logarithmic region with $A_1 = A_2/2$ in previous study of TBL (Marusic et al. 2017). This relation was observed at also pipe flow in present study as $0.72 = 1.44/2$ (Fig. 5(a)) by taking account to LDV specific issues such as the fringe distortion which affects the outer region and the spatial resolution which affects the inner region at high Reynolds number.

CONCLUSION

LDV measurement parameters which influence turbulence intensity such as the spatial resolution and the fringe distortion are evaluated by supporting of the wire rotary device and it is reflected to the measurement results by each correction methods.

Reynolds number dependence of the streamwise inner peak showed consistency with Eq. (7) and Eq. (8), and good agreement with previous experimental results of TBL rather than pipe flows. The consistency indicates possibility that the streamwise inner peak values independence of the geometry.

On, the turbulence intensity profiles of 3 components indicate clearly the logarithmic regions for $Re_\tau > 11200$, these positions are same between streamwise and spanwise component ($y/R = 0.05\sim 0.25$), but different with the wall-normal component ($y/R = 0.015\sim 0.07$). These profiles agree well DNS data at low Reynolds number and previous experimental data at high Reynolds number.

Moreover, the relation between the Reynolds number dependence of streamwise inner peak and the logarithmic region derived by the attached addy hypothesis, which is $A_1 = A_2/2$, was observed at also pipe flow in present study. We should emphasize that these results are based on a carefully taking account of LDV specific problems such as the fringe distortion and the spatial resolution.

REFERENCES

- Ahn, J., Lee, J. H., Lee, J., Kang, J., & Sung, H. J., 2015, "Direct numerical simulation of a 30R long turbulent pipe flow at $Re_\tau=3008$ ", *Physics of Fluids*, 27(6), 065110.
- Chen, X., Sreenivasan, K.R., 2020, "Reynolds number scaling of the peak turbulence intensity in wall flows", *J. Fluid Mech.*, pp. 1–11.
- Chin, C., Monty, J. P., & Ooi, A., 2014, "Reynolds number effects in DNS of pipe flow and comparison with channels and boundary layers", *International Journal of Heat and Fluid Flow*, 45(1), pp. 33–40.
- Durst, F., Jovanović, J., Sender, J., 1995, "LDA measurements in the near-wall region of a turbulent pipe flow", *J. Fluid Mech.*, 295, pp. 305–335.
- Furuichi, N., Terao, Y., Wada, Y., & Tsuji, Y., 2015, "Friction factor and mean velocity profile for pipe flow at high Reynolds numbers", *Physics of Fluids*, 27(9).
- Hultmark, M., Vallikivi, M., Bailey, S. C. C., Smits, A. J., 2012, "Turbulent pipe flow at extreme reynolds numbers", *Physical Review Letters*, 108(9).

Marusic, I., Chauhan, K. A., Kulandaivelu V., and Hutchins N., 2015 "Evolution of zero-pressure-gradient boundary layers from different tripping conditions," *J. Fluid Mech.* 783, pp. 379–411.

Marusic, I., Baars, W.J., Hutchins, N., 2017, "Scaling of the streamwise turbulence intensity in the context of inner-outer interactions in wall turbulence", *Phys. Rev. Fluids*, 2-10, pp. 1–22.

Ono, M., Furuichi, N., Kurihara N., Wada Y., Tsuji, Y., 2022, "Reynolds number dependence of inner peak turbulence intensity in pipe flow", *Physics of Fluids*, 34.

Perry, A. E., & Chong, M. S., 1982, "On the mechanism of wall turbulence", *J. Fluid Mech.*, 119, 173–217.

Pirozzoli, S., Romero, J., Fatica, M., Verzicco, R., Orlandi, P., 2021, "One-point statistics for turbulent pipe flow up to $Re_\tau=6000$. *Journal of Fluid Mechanics*", 926, pp. 1–20.

Samie, M., Marusic, I., Hutchins, N., Fu, M. K., Fan, Y., Hultmark, M., Smits, A. J., 2018, "Fully resolved measurements of turbulent boundary layer flows up to $Re_\tau=20000$ ", *J. Fluid Mech.*, 851, pp. 391–415.

Willert, C. E., Soria, J., Stanislas, M., Klinner, J., Amili, O., Eisfelder, M., Cuvier, C., Bellani, G., Fiorini, T., Talamelli, A., 2017, "Near-wall statistics of a turbulent pipe flow at shear Reynolds numbers up to 40 000", *J. Fluid Mech.*, 826, pp. 1–10.

Yamamoto, Y., & Tsuji, Y., 2018, "Numerical evidence of logarithmic regions in channel flow at $Re_\tau=8000$ ", *Physical Review Fluids*, 3(1), pp. 1–10.

Zanoun, E. S., Egbers, C., Örlü, R., Fiorini, T., Bellani, G., & Talamelli, A., 2019, "Experimental evaluation of the mean momentum and kinetic energy balance equations in turbulent pipe flows at high Reynolds number". *Journal of Turbulence*, 20(5), pp 285–299.

Zhao, R., & Smits, A. J., 2007, "Scaling of the wall-normal turbulence component in high-Reynolds-number pipe flow", *J. Fluid Mech.*, 576, pp 457–473.